# Dalton Transactions

Accepted Manuscript

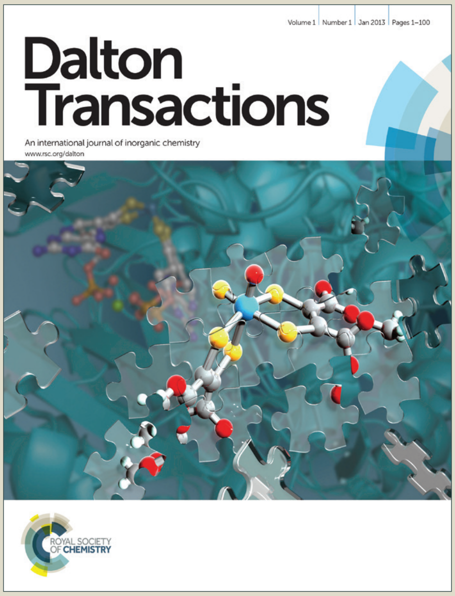

ROYAL SOCIETY OF CHEMISTRY

www.rsc.org/dalton

# Axial Bonded Pentads Constructed on Sn(IV) Porphyrin Scaffold

**Yogita Pareek, Vellanki Lakshmi and Mangalampalli Ravikanth***

Department of Chemistry, Indian Institute of Technology Bombay, Powai,

Mumbai 400 076, India. E-mail: ravikanth@chem.iitb.ac.in

## Abstract

Three covalently linked dyads such as porphyrin-ferrocene, porphyrin-BODIPY and porphyrin-sapphyrin containing one hydroxyphenyl group at *meso*-position of porphyrin were synthesized by coupling of *trans*-functionalized porphyrin building block, 5-(4-hydroxyphenyl)-10-(4-iodophenyl)-15,20-diphenyl porphyrin with ethynyl functionalized redox/chromophore building block under mild Pd(0) coupling conditions. The dyads were then reacted with SnTTP$(OH)_2$ in benzene in 2:1 ratio at reflux temperature for 12 hours followed by simple alumina column chromatographic purification which afforded three pentads containing three different types of redox/chromophore components in 62-89 % yields. The pentads are very stable and freely soluble in all common organic solvents. The pentads formation was confirmed by MALDI-TOF mass spectrometry and 1D and 2D NMR studies. Absorption and electrochemical studies suggested that the three components in pentads retain their independent characteristic features without significant alterations in their properties thus acting like supramolecular assemblies. The steady state fluorescence studies indicated a possibility of energy/electron transfer among the three types of components in pentads.

# Axial Bonded Pentads Constructed on Sn(IV) Porphyrin Scaffold

**Yogita Pareek, and Mangalampalli Ravikanth***

Department of Chemistry, Indian Institute of Technology Bombay, Powai,

Mumbai 400 076, India. E-mail: ravikanth@chem.iitb.ac.in

## Introduction

Axial bonded multiporphyrin arrays can be generated when the porphyrin cavity possesses a metal ion which has at least one axial site available for coordination.[1-13] Since many of the metalloporphyrins do not show specific selectivity toward one particular type of donor, it becomes difficult to design and construct multiporphyrin arrays with desired specifications. However, an extensive work carried out over the period on metalloporphyrin based assemblies suggest that porphyrins containing nitrogen donor ligands such as pyridyl, imidazole, pyrazole, amine on their periphery prefer to coordinate with Zn(II), Ru(II), Os(II), Mg(II), Rh(III) porphyrins whereas the porphyrins with oxygen donors such as carboxylates and aryloxides on periphery prefer to coordinate with Fe(III), Mn(III), Al(III), Sn(IV) porphyrins to form axial bonded multiporphyrin arrays.[14-18] Among oxophilic metalloporphyrins, Sn(IV) porphyrins have very strong affinity toward oxygen donor ligands and are ideal scaffolds for the construction of axial bonded assemblies because of their novel spectral and electrochemical properties.[19] Sn(IV) porphyrins are very stable diamagnetic compounds with NMR active Sn(IV) nuclei which helps in structural characterization. Thus, Sn(IV) porphyrins have many advantageous properties to be used as scaffolds for the synthesis of axial bonded assemblies.[19,20] Inspite of several favourable characteristics, the reports on Sn(IV) porphyrin based axial-bonded assemblies are, surprisingly, rather limited[21-32] and additional examples on Sn(IV) porphyrin based assemblies would help in exploring their use as new materials for diverse applications.

Herein we report synthesis and characterization of three Sn(IV) porphyrin based pentads **1-3** containing covalently linked porphyrin-ferrocene, porphyrin-BODIPY and porphyrin-sapphyrin dyads as axial ligands. The covalently linked dyads containing *meso*-hydroxyphenyl group on porphyrin were synthesized by coupling of appropriate building blocks under Pd(0) coupling conditions and the dyads were then reacted with Sn(IV) porphyrin in benzene to generate stable Sn(IV) porphyrin based pentads in decent yields. The spectral, electrochemical and photophysical properties of these novel pentads and their reference compounds are described.

## Result and discussion

To synthesize the desired axially bonded Sn(IV) porphyrin based pentads **1-3**, we need an access to the covalently linked dyad building blocks such as porphyrin-ferrocene dyad **4**, porphyrin-BODIPY dyad **5** and porphyrin-sapphyrin dyad **6** containing one hydroxyphenyl group at the *meso*-position of porphyrin which were synthesized as shown in Scheme 1. The desired *trans*-functionalized porphyrin building block, 5-(4-hydroxyphenyl)-10-(4-iodophenyl)-15,20-diphenyl porphyrin[33] **7** and the other required precursors α-ethynyl ferrocene **8**, *meso*-(*p*-ethynylphenyl) BODIPY[34] **9**, 5-(4-ethynylphenyl)-10,15,20-tris(4-tolyl)-25,27,29-trithiasapphyrin[35] **10** and SnTTP$(OH)_2$[36] **11** were prepared by following the literature procedures. The dyads **4-6** were prepared by coupling of ferrocene/BODIPY/sapphyrin building blocks containing ethynyl functional group with *trans*-functionalized porphyrin building block **7** in toluene/triethylamine in the presence of catalytic amounts of $AsPh_3$ and $Pd_2(dba)_3$ at 40 °C for 6-8 h. Column chromatographic purification on silica afforded pure covalently linked dyads **4-6** in 67-73% yields. The corresponding molecular ion peak in ES-MS mass spectra confirmed the identities of the dyads **4-6**. In $^1$H NMR spectra of dyads **4-6**, the resonances corresponding to both the moieties were present with no significant changes in their chemical shifts compared to their corresponding constituted monomers. The comparison of $^1$H NMR spectra of porphyrin-BODIPY dyad **5** along with its constituted monomers *meso*-(*p*-ethynylphenyl) BODIPY **9** and *trans*-functionalized porphyrin building block **7** is shown in Figure 1. As shown in Figure 1, the BODIPY monomer **9** exhibit three sets of resonances at 6.55, 6.91 and 7.95 ppm for six pyrrole protons where as the eight pyrrole protons of porphyrin monomer **7** were appeared as multiplet in 8.85-8.87 ppm region. However, in dyad **5**, the six pyrrole protons of BODIPY moiety appeared as three sets of signals at 6.60, 7.01 and 7.97 ppm and the porphyrin eight pyrrole protons appeared as multiplet in 8.86-8.90 ppm region with almost no changes in their chemical shifts compared to monomers indicating that the two moieties in dyad **5** interact very weakly and retain their individual characteristic features. Similar observations were made for dyads **4** and **6**.

The pentads **1-3** were prepared by treating one equivalent of SnTTP$(OH)_2$ **11** with two equivalents of appropriate dyad **4-6** in benzene at reflux temperature for 12 h. The crude compounds obtained after removal of solvent on rotary evaporator under vacuum were subjected to alumina column chromatography and afforded pentads in 62-80% yields. The pentads **1-3** were characterized by NMR, absorption, electrochemistry and fluorescence spectroscopic techniques. The MALDI-TOF mass spectra showed a strong peak corresponding to M-(O-axial dyad) for pentads **1-3**. However, $^1$H NMR and $^1$H-$^1$H COSY NMR techniques were very useful to arrive at the structure of these compounds. The proton assignments of pentads **1-3** were made on the basis of the resonance position and integrated intensity data as well as the proton-to-proton connectivity information revealed in the $^1$H-$^1$H COSY NMR. The comparison of $^1$H NMR spectra of pentad **1** along with its constituted moieties, dyad **4** and SnTTP$(OH)_2$ **11** is presented in Figure 2 along with $^1$H-$^1$H COSY NMR spectrum of pentad **1**. The close inspection of $^{1}$H NMR spectra of pentads **1-3** revealed that certain protons of basal Sn(IV) porphyrin and porphyrin moiety in axial dyad experienced shifts due to ring current effect of adjacent porphyrins and appeared at different region as compared to their corresponding monomeric units. For example, in pentad **1**, the eight β-pyrrole protons of basal Sn(IV) porphyrin moiety appeared as multiplet in 9.39-9.41 ppm region which were downfield shifted compared to SnTTP$(OH)_2$ **11** in which the eight β-pyrrole protons resonate as singlet at 9.40 ppm. On the other hand, the β-pyrrole protons of porphyrin moiety of axial porphyrin-ferrocene dyad of pentad **1** appeared as three sets of resonances at 8.14, 8.57 and 8.82 ppm which were upfield shifted compared to porphyrin moiety in dyad **4** in which the β-pyrrole protons were appeared as one multiplet in 8.85-8.87 ppm region. In pentad **1**, the two β-pyrrole protons of *type a* and two β-pyrrole protons of *type b* of porphyrin unit of axial dyads which are facing Sn(IV) porphyrin were appeared as two sets of doublets at 8.14 ppm and 8.57 ppm respectively and these doublets were identified based on cross-peak connectivity observed in $^{1}$H-$^{1}$H COSY spectrum. The other four β-pyrrole protons of *type c* of porphyrin moiety in axial dyad in pentad **1** appeared as multiplet in 8.82-8.84 ppm region. Thus, in pentad **1**, the *type a* and *type b* pyrrole protons which are facing the Sn(IV) porphyrin unit experienced more upfield shifts and the *type c* protons which are away from the Sn(IV) porphyrin unit experienced slight upfield shifts compared to β-pyrrole protons of porphyrin unit in corresponding porphyrin-ferrocene dyad **4**. The ferrocenyl protons of axial dyad in pentad **1** which are very far away from Sn(IV) porphyrin unit did not show any shifts compared to ferrocenyl protons in dyad **4**. However, the formation of pentad **1** was more clearly evident in the large upfield shifts observed for the protons of *meso*-phenoxo group of porphyrin unit in axial dyad that is bound to Sn(IV) center. These protons being affected by both the inherent deshielding effect of porphyrin moiety of axial dyad and the shielding effect of the basal

Sn(IV) porphyrin, resonate at upfield region in pentad **1**. The 3,5-protons of *meso*-phenoxo group which appeared as doublet at 7.88 ppm in dyad **4** shifted to upfield and appeared as doublet at 6.58 ppm in pentad **1**. Similarly, the 2,6-protons of *meso*-phenoxo group which appeared as doublet at 7.21 ppm in dyad **4** were shifted to 2.44 ppm in pentad **1** due to large ring current effect of basal Sn(IV) porphyrin experienced by these protons in pentad **1**. The upfield shifts of protons of *meso*-phenoxo group of porphyrin moiety of axial dyad unit was further confirmed by the proton-proton connectivity pattern observed by $^1$H-$^1$H COSY spectrum shown in Figure 2b. The pentads **2** and **3** also showed similar shifts in the chemical shifts of basal Sn(IV) porphyrin and porphyrin moiety of axial porphyrin-BODIPY dyad in pentad **2** and porphyrin-sapphyrin dyad in pentad **3**. Thus NMR studies clearly supports the formation of pentads **1-3**.

## Absorption, electrochemical and fluorescence studies

The properties of pentads **1-3** and their associated reference dyads **4-6** and monomeric compounds were studied using absorption, electrochemical and fluorescence techniques. The comparison of absorption spectra of pentads **1-3** and 1:1 mixture of their correspondining reference units, recorded in $CH_2Cl_2$ is presented in Figure 3 and absorption data of all compounds are tabulated in Table 1. The absorption spectra of pentads showed features of their constituted monomers with negligible shifts in their peak maxima. For example, pentad **3** (figure 3c) showed eight absorption bands with absorption peak maxima at 423, 429, 513, 555, 601, 651, 682 and 882 nm. In this, the bands at 423 and 651 nm are mainly due to porphyrin unit; the bands at 429, 555 and 601 nm are due to Sn(IV) porphyrin and the bands at 513, 682 and 882 nm are mainly due to sapphyrin unit. The corresponding 1:1 mixture of porphyrin-sapphyrin dyad **6** and SnTTP(OH)$_2$ **11** also showed similar absorption features. However, the extinction coefficients of absorption bands of pentad **3** were larger compared to its 1:1 mixture of constituted units indicating that pentad **3** is intact in solution and also exhibit weak interaction among the components. Similar features were noted for pentads **1** and **2**. Thus, absorption study of pentads **1-3** indicated that the components in pentads retain their independent absorption features with minimum perturbation and acts like supramolecular assemblies.

The electrochemical studies were carried out on pentads **1-3** and dyads **4-6** along with their corresponding monomers in $CH_2Cl_2$ using TBAP as supporting electrolyte and the data are presented in Table 2. The reduction waves of pentads **2** and **3** are shown in Figure 4. The redox potential data of dyads **4-6** and pentads **1-3** were analyzed based on the data of their corresponding monomers. The inspection of data presented in Table 2 indicated that the redox potentials of pentads **1-3** are in the same range as those of their corresponding dyads **4-6** and monomers. For example, the pentad **2** showed three oxidations at 1.01, 1.27 and 1.42 V and five reductions at -0.73, -0.99, -1.25, -1.40 and -1.58 V. In this, the oxidations 1.01 and 1.27 V were mainly due to $N_4$-porphyrin and the oxidation at 1.42 V was due to Sn(IV) porphyrin unit. On the other hand, the reduction at -0.73 V was exclusively for BODIPY unit; the reductions at -0.99 and -1.40 V were due to Sn(IV) porphyrin unit; the reduction at -1.25 V was exclusively from $N_4$-porphyrin unit and reduction potential at -1.58 V was because of both $N_4$-porphyrin and BODIPY units. Similarly, the redox potentials of pentads **1** and **3** were also assigned on the basis of the redox data of their constituted monomers. The redox properties of pentads **1-3** did not alter much as compared to their monomers which support weak interaction among the components in pentads **1-3**.

The steady state fluorescence properties of pentads **1-3**, dyads **4-6** and the relevant monomers were studied at different excitation wavelengths and the data are presented in Table 3.

The dyad **4** containing covalently linked ferrocene and porphyrin units, upon excitation at 515 nm where porphyrin unit absorbs exclusively, the emission from porphyrin was quenched by 99% which is attributed to photoinduced electron transfer from ferrocene unit to porphyrin. However, the dyad **5**, on excitation at 488 nm where BODIPY unit absorbs strongly, the emission from BODIPY was quenched by 99% and strong emission from porphyrin unit was observed with a quantum yield matching with reference $H_2$TPP. The excitation spectrum of dyad **5** recorded at 660 nm matched closely with its absorption spectrum. These results indicated that in dyad **5**, there is an efficient energy transfer from BODIPY unit to porphyrin unit. Interestingly, in dyad **6**, the sapphyrin unit is non-emissive but its excited state is lower than porphyrin. Thus, upon excitation of dyad **6** at 515 nm where porphyrin unit absorbs strongly, the emission from porphyrin unit was quenched by 89% because of energy/electron transfer to the sapphyrin unit which was then dissipated non-radiatively. Thus, except dyad **5**, the porphyrin emission from other two dyads was significantly quenched. The fluorescence properties of pentads **1-3** were studied in comparison with 1:1 mixture of corresponding dyad and Sn(IV) porphyrin. The comparison of fluorescence spectra of pentads **1-3** with their corresponding 1:1 mixture of dyad and SnTTP$(OH)_2$ **11** recorded using excitation wavelength of 560 nm where Sn(IV) porphyrin absorbs strongly is presented in Figure 5. In all three pentads **1-3**, upon excitation at 560 nm where Sn(IV) porphyrin unit absorbs strongly, the emission from Sn(IV) porphyrin is weak but relatively strong emission was observed from porphyrin unit which was axially bonded to Sn(IV) center. On the other hand, upon excitation of their corresponding 1:1 mixture at 560 nm, we noted emission mainly from Sn(IV) porphyrin unit. These results supports energy transfer from Sn(IV) porphyrin unit to porphyrin unit in all pentads **1-3**. However, as shown in the Table 3, the quantum yield of porphyrin unit in all three pentads **1-3** was very low which can be rationalized as follows: In pentad **1**, upon excitation at 560 nm where Sn(IV) porphyrin is the strong absorber as well as at 515 nm where porphyrin unit is the strong absorber, the fluorescence of porphyrin unit was quenched by ~90% because of its coordination with heavy Sn(IV) ion and also due to redox active ferrocene group . In pentad **2**, the excitation of BODIPY at 488 nm as well as excitation at Sn(IV) porphyrin at 560 nm resulted in energy transfer to the porphyrin unit. However, the porphyrin emission is weak in pentad **2** due to its coordination with Sn(IV) porphyrin. In pentad **3**, the excitation of Sn(IV) porphyrin at 560 nm resulted in energy transfer from Sn(IV) porphyrin unit to porphyrin unit which was further transferred to sapphyrin unit and ultimately dissipated non-radiatively leading to weak porphyrin fluorescenc. Thus, the steady state fluorescence studies indicated a possibility of energy/electron transfer among the components in pentads **1**-**3**.

## Conclusions

In conclusion, we synthesized three covalently linked dyads such as porphyrin-ferrocene, porphyrin-BODIPY and porphyrin-sapphyrin dyads containing one hydroxyphenyl group at *meso* position of porphyrin by coupling of *trans*-porphyrin building block with functionalized redox active or chromophore building blocks under standard Pd(0) coupling conditions in high yields. The dyads were reacted with $SnTTP(OH)_2$ in benzene at reflux temperature in 2:1 ratio and afforded pentads containing three different types of redox/optically active components in decent yields. Mass and NMR studies confirmed the formation of pentads. Absorption and electrochemical studies supported weak interaction among the components in pentads. The fluorescence studies indicated a possibility of electron/energy transfer among the constituted components in pentads. The material properties of these pentads are presently under investigation.

## Experimental Section

**General synthesis of dyads 4-6:** A solution of one equivalent of 5-(4-hydroxyphenyl)-10-(4-iodophenyl)-15,20-diphenyl porphyrin **7**, and one equivalent of α-ethynyl ferrocene **8** or *meso*-(*p*-ethynylphenyl) BODIPY **9** or 5-(4-ethynylphenyl)-10,15,20-tris(4-tolyl)-25,27,29-trithiasapphyrin **10** in dry toluene/triethyleamine (3:1) was purged with nitrogen for 15 min. The coupling was initiated by adding $AsPh_3$ (1.2 equivalent) followed by $Pd_2(dba)_3$ (0.15 equivalent) and the reaction mixture was stirred at 40 °C for 6-8 h. TLC analysis indicated the appearance of new spot apart from the small amount of corresponding unreacted monomers. The crude reaction mixture was purified by silica column chromatography using petroleum ether/dichloromethane as eluent. The excess $AsPh_3$ and small amounts of unreacted monomers were removed using petroleum ether/dichloromethane (80:20) and the dyads **4-6** were collected using petroleum ether/dichloromethane (50:50).

**Porphyrin-ferrocene dyad 4**: Yield 70%. M.P. > 300 °C. $^1$H NMR (400 MHz, $CDCl_3$): $\delta$ = −2.78 (s, 2H, NH), 4.33 (s, 2H, Ferrocene), 4.36 (s, 5H, Ferrocene), 4.64 (s, 2H, Ferrocene), 7.21 (d, $J$ = 8.0 Hz, 2H, Ar, type 2,6), 7.75 (m, 6H, Ar), 7.88 (d, $J$ = 7.7 Hz, 2H, Ar, type 3,5), 8.05 (d, $J$ = 7.9 Hz, 2H, Ar), 8.21 (d, $J$ = 7.7 Hz, 6H, Ar), 8.87 (m, 8H, β-pyrrole) ppm. ES-MS mass: $C_{56}H_{38}FeN_4O$ calcd. av. mass 838.7 obsd m/z 839.3 [$M^+$+1]. UV-Vis (in $CH_2Cl_2$, $\lambda_{max}$/nm, ε/$mol^{-1}$ $dm^3$ $cm^{-1}$): 418 (6.24), 516 (4.33), 552 (4.06), 592 (3.79), 648 (3.86). Elemental analysis calcd (%): C 80.19, H 4.57, N 6.68; found C 80.22, H 4.61, N 6.70.

**Porphyrin-BODIPY dyad 5:** Yield 73 %. M.P. > 300 °C. $^1$H NMR (400 MHz, CDCl$_3$): $\delta$ = -2.90 (s, 2H, NH), 6.60 (d, *J* = 4.3 Hz, 2H, BODIPY Pyrrole), 7.01 (d, *J* = 3.9 Hz, 2H, BODIPY Pyrrole), 7.20 (d, *J* = 7.4 Hz, 2H, Ar, type 2,6), 7.65 (d, *J* = 8.4 Hz, 2H, Ar, type 3,5), 7.75-7.83 (m, 8H, Ar), 7.97 (d, *J* = 4.8 Hz, 2H, BODIPY Pyrrole), 8.03-8.07 (m, 4H, Ar), 8.20-8.25 (m, 6H, Ar), 8.86-8.90 (m, 8H, Por Pyrrole) ppm. ES-MS mass: $C_{61}H_{39}BF_2N_6O$ calcd. av. mass 920.8 obsd m/z 921.2 [M$^+$+1]. UV-Vis (in CH$_2$Cl$_2$, $\lambda_{max}$/nm, ε/mol$^{-1}$ dm$^3$ cm$^{-1}$): 420 (6.36), 552 (4.01), 552 (4.06), 593 (3.70), 649 (3.65). Elemental analysis calcd (%): C 79.57, H 4.27, N 9.13; found C 79.60, H 4.29, N 9.17.

**Porphyrin-sapphyrin dyad 6:** Yield 67 %. M.P. > 300 °C. $^1$H NMR (400 MHz, CDCl$_3$): $\delta$ = -2.75 (s, 2H, NH), -0.67 (d, *J* = 5.4 Hz, 1H, inverted thiophene), -0.63 (d, *J* = 5.4 Hz, 1H, inverted thiophene), 2.66 (s, 3H, tolyl CH$_3$), 2.74 (s, 6H, tolyl CH$_3$), 7.22 (d, *J* = 7.1 Hz, 2H, Ar, type 2,6), 7.52 (d, *J* = 7.6 Hz, 2H, Ar), 7.60 (d, *J* = 7.7 Hz, 2H, Ar), 7.69-7.74 (m, 4H, Ar), 7.76-7.80 (m, 8H, Ar), 8.04 (d, *J* = 8.4 Hz, 2H, Ar), 8.09 (d, *J* = 8.2 Hz, 2H, Ar, type 3,5), 8.22-8.24 (m, 6H, Ar), 8.28 (d, *J* = 8.1 Hz, 2H, Ar), 8.32 (d, *J* = 8.0 Hz, 2H, Ar), 8.46 (d, *J* = 7.9 Hz, 2H, Ar), 8.58 (d, *J* = 4.4 Hz, 1H, Sap Pyrrole), 8.60 (d, *J* = 4.3 Hz, 1H, Sap Pyrrole), 8.67 (d, *J* = 4.3 Hz, 1H, Sap Pyrrole), 8.70 (d, *J* = 4.3 Hz, 1H, Sap Pyrrole), 8.85 (d, *J* = 4.2 Hz, 2H, Por Pyrrole), 8.90-8.91 (m, 6H, Por Pyrrole), 9.80-9.81 (m, 2H, β-thiophene), 10.21 (d, *J* = 4.9 Hz, 2H, β-thiophene) ppm. ES-MS mass: $C_{97}H_{64}N_6OS_3$ calcd. av. mass 1425.7 obsd m/z 1426.2 [M$^+$+1]. UV-Vis (in CH$_2$Cl$_2$, $\lambda_{max}$/nm, ε/mol$^{-1}$ dm$^3$ cm$^{-1}$): 418 (5.31), 513 (4.33), 550 (3.95), 591 (3.73), 647 (3.65), 678 (3.56), 882 (3.45). Elemental analysis calcd (%): C 81.71, H 4.52, N 5.89; found C 81.74, H 4.56, N 5.93.

**General synthesis for pentads 1-3:** The pentads **1-3** were synthesized by refluxing one equivalent of Sn(IV)TTP$(OH)_2$ **11** with two equivalent of appropriate dyad **4/5/6** in dry benzene for 12 hours under nitrogen atmosphere. The solvent was evaporated under reduced pressure and the resulted residue was subjected to alumina column chromatography. The desired product was eluted with pet ether/dicholoromethane (30:70) and was recrystallized using dichloromethane/*n*-hexane mixture to afford pentads **1-3** in 62-80 % yields.

**Pentad 1:** Yield 80 %. $^1$H NMR (400 MHz, $CDCl_3$): $\delta$ = -2.93 (s, 4H, NH), 2.44 (d, *J* = 8.3 Hz, 4H, phenoxo, type 2,6), 2.62 (s, 12H, $CH_3$), 4.33 (s, 4H, Ferrocene), 4.35 (s, 10H, Ferrocene), 4.64 (s, 4H, Ferrocene), 6.58 (d, *J* = 8.3 Hz, 4H, phenoxo, type 3,5), 7.48 (d, *J* = 7.8 Hz, 8H, Ar), 7.71-7.77 (m, 16H, Ar), 8.14-8.19 (m, 16H, 4+12, pyrrole type a + Ar), 8.33 (d, *J* = 7.7 Hz, 8H, Ar), 8.57 (d, *J* = 4.6 Hz, 4H, pyrrole, type b), 8.82-8.84 (m, 8H, pyrrole, type c), 9.39-9.41 (m, 8H, SnP Pyrrole) ppm. UV-Vis (in $CH_2Cl_2$, $\lambda_{max}$/nm, ε/mol$^{-1}$ dm$^3$ cm$^{-1}$): 420 (6.15), 430 (6.08), 517 (4.67), 560 (4.65), 602 (4.44), 650 (4.17). MALDI-TOF MS: m/z: calcd ($M^+$) 2463.0; found 1624 ($M^+$-$C_{56}H_{38}FeN_4O$).

**Pentad 2:** Yield 73 %. $^1$H NMR (400 MHz, $CDCl_3$): $\delta$ = -2.92 (s, 4H, NH), 2.42 (d, *J* = 8.3 Hz, 4H, phenoxo, type 2,6), 2.62 (s, 3H, $CH_3$), 2.64 (s, 6H, $CH_3$), 2,68 (s, 3H, $CH_3$), 6.59 (d, *J* = 8.1 Hz, 8H, 4+4, phenoxo type 3,5 + BODIPY pyrrole), 7.01 (d, *J* = 4.0 Hz, 4H, BODIPY pyrrole), 7.50 (d, *J* = 8.2 Hz, 8H, Ar), 7.66 (d, *J* = 8.2 Hz, 4H, Ar), 7.75-7.79 (m, 12H, Ar), 7.83 (d, *J* = 8.2 Hz, 4H, Ar), 7.94-7.98 (m, 8H, 4+4, BODIPY pyrrole + Ar), 8.12-8.26 (m, 16H, 4 + 12, Por Pyrrole type a + Ar), 8.33-8.36 (m, 8H, Ar), 8.59 (d, *J* = 4.6 Hz, 4H, Por Pyrrole, type b), 8.80-8.93 (m, 8H, Por Pyrrole, type c), 9.31 (d, *J* = 5.0 Hz, 2H, SnP Pyrrole), 9.42 (s, 4H, SnP

Pyrrole), 9.48 (d, *J* = 5.0 Hz, 2H, SnP Pyrrole) ppm. UV-Vis (in $CH_2Cl_2$, $\lambda_{max}$/nm, ε/mol$^{-1}$ dm$^3$ cm$^{-1}$): 421 (6.02), 431 (5.82), 506 (4.93), 557 (4.50), 599 (4.22), 649 (3.96). MALDI-TOF MS: m/z: calcd ($M^+$) 2627.1; found 1707.3 ($M^+$-$C_{61}H_{38}BF_2N_6O$).

**Pentad 3:** Yield 62 %. $^1$H NMR (400 MHz, $CDCl_3$): $\delta$ = -2.90 (s, 4H, NH), -0.62 (d, *J* = 5.40 Hz, 2H, inverted thiophene), -0.63 (d, *J* = 5.4 Hz, 2H, inverted thiophene), 2.44 (d, *J* = 7.9 Hz, 4H, phenoxo type 2,6), 2.56 (s, 6H, tolyl $CH_3$), 2.62 (s, 6H, tolyl $CH_3$), 2.64 (s, 6H, tolyl $CH_3$), 2.71 (s, 6H, tolyl $CH_3$), 2.74 (s, 6H, tolyl $CH_3$), 6.59 (d, *J* = 7.7 Hz, 4H, phenoxo type 3,5), 7.50-7.51 (m, 10H, Ar), 7.63 (d, *J* = 7.7 Hz, 8H, Ar), 8.03 (d, *J* = 8.7 Hz, 8H, Ar), 8.06 (d, *J* = 8.7 Hz, 8H, Ar), 8.17-8.30 (m, 28H, Ar), 8.32 (d, *J* = 8.7 Hz, 6H, Ar), 8.34-8.37 (m, 8H, Ar), 8.47-8.50 (m, 4H, pyrrole, type a), 8.57-8.66 (m, 8H, 4+4, pyrrole sap + type b), 8.67 (d, *J* = 4.3 Hz, 2H, pyrrole sap), 8.71 (d, *J* = 4.4 Hz, 2H, Pyrrole sap), 8.84-8.87 (m, 8H pyrrole, type c), 9.41 (d, *J* = 4.3 Hz, 8H, SnP Pyrrole), 9.80 (d, *J* = 4.9 Hz, 4H, *β*-thiophene), 10.21 (d, *J* = 4.9 Hz, 4H, *β*-thiophene) ppm. UV-Vis (in $CH_2Cl_2$, $\lambda_{max}$/nm, ε/mol$^{-1}$ dm$^3$ cm$^{-1}$): 423 (6.13), 429 (6.06), 513 (5.74), 555 (4.52), 601 (4.32), 651 (4.24), 682 (4.42), 882 (3.83). MALDI-TOF MS: m/z: calcd ($M^+$) 3637.1; found 2212 ($M^+$-$C_{97}H_{63}N_6OS_3$).

**Acknowledgement:** M.R. thanks Department of Science and Technology (DST) for financial support. Y.P. thanks Council of Scientific and Industrial Research (CSIR) for senior research fellowship.

**Supporting Information Available:** (see footnote on the first page of this article): The characterization data including mass, $^1$H NMR for all the compounds.

## References:

1. Kumar, P. P.; Premaladhaand, G.; Maiya, B. G. *Chem. Commun.* **2005**, 3823.
2. Reddy, D. R.; Maiya, B. G. *Chem. Commun.* **2001**, 117.
3. Rao, T. A.; Maiya, B. G. *Inorg. Chem.* **1996**, *35*, 4829.
4. Davidson, G. J. E.; Lane, L. A.; Raithby, P.R.; Warren, J.E.; Robinson, C.V.; Sanders, J. K. M. *Inorg. Chem.* **2008**, *47*, 8721.
5. Xu, T.; Lu, R.; Liu, X.; Zheng, X.; Qiu, X.; Zhao, Y. *Org. Lett*. **2007**, *9*, 797.
6. P. P. Kumar and B. G. Maiya, *New J. Chem.,* 2003, 27, 619.
7. G. J. E. Davidson, L. H. Tong, P. R. Raithby and J. K. M. Sanders, *Chem. Commun.,* **2006**, 3087.
8. G. A. Metselaar, J. K. M. Sanders and J. de Mendoza, *Dalton Trans.,* **2008**, 588.
9. E. Iengo, G. D. Pantosx, J. K. M. Sanders, M. Orlandi, C. Chiorboli, S. Fracassoc and F. Scandola, *Chem. Sci.*, **2011**, *2*, 676.
10. A. Ghosh, D. K. Maity, M. Ravikanth, *New. J. Chem.* **2012**, *36*, 2630-2641.
11. Michelsen, U.; Hunter, C. A. *Angew. Chem., Int. Ed.* **2000**, *39*, 764.
12. Tsuda, A.; Nakamura, T.; Sakamoto, S.; Yamaguchi, K.; Osuka, A. *Angew. Chem., Int. Ed.* **2002**, *41*, 2817.
13. Furutsu, D.; Satake, A.; Kobuke, Y. *Inorg. Chem.* **2005**, *44*, 4460.
14. Wojaczynski, J.; Latos-Grazynski, L. *Coord. Chem. Rev.* **2000**, *204*, 113.
15. Scandola, F.; Chiorboli, C.; Prodi, A.; Iengo, E.; Alessio, E. *Coord. Chem. Rev.* **2006**, *250*, 1471-1496.
16. Iengo, E.; Zangrando, E. Alessio, E. *Acc. Chem. Res.* **2006**, *39*, 841-851.

17. Prodi, A.; Indelli, M. T.; Kleverlaan, C. J.; Alessio, E.; Scandola, F. *Coord. Chem. Rev.* **2002**, *229*, 51-58.

18. Imamura, T.; Fukushima, K. *Coord. Chem. Rev.* **2000**, *198*, 133-156.

19. Arnold, D. P.; Blok, J. *Coord. Chem. Rev.* **2004**, *248*, 299 and references cited therein.

20. Shetti, V. S.; Pareek, Y.; Ravikanth, M. *Coord. Chem. Rev.* **2012**, *256*, 2816.

21. Giribabu, L.; Rao, T. A.; Maiya, B. G. *Inorg. Chem.* **1999**, *38*, 4971.

22. Shetti, V. S.; Ravikanth, M. *Inorg. Chem.* **2010**, *49*, 2692.

23. Honda, T.; Nakanishi, T.; Ohkubo, K; Kojima, T.; Fukuzumi, S. *J. Phys. Chem. C* **2010**, *114*, 14290.

24. Kumar, A. A.; Giribabu, L.; Reddy, R. D.; Maiya, B. G. *Inorg. Chem.* **2001**, *40*, 6757.

25. Kim, H. J.; Bampos, N.; Sanders, J. K. M. *J. Am. Chem. Soc.* **1999**, *121*, 8120.

26. Redman, J. E.; Feeder, N.; Teat, S. J.; Sanders, J. K. M. *Inorg. Chem.* **2001**, *40*, 2486.

27. Maiya, B. G.; Bampos, N.; Kumar, A. A.; Feeder, N.; Sanders, J. K. M. *New J. Chem.* **2001**, *25*, 797.

28. Fallon, G. D.; Langford, S. J.; Lee, M. A. –P.; Lygris, E. *Inorg. Chem. Commun.* **2002**, *5*, 715.

29. Langford, S. J.; Woodward, C. P. *Collect. Czech. Chem. Commun.* **2004**, *69*, 996.

30. Hunter, C. A.; Tomas, S. *J. Am. Chem. Soc.* **2006**, *128,* 8975.

31. Metselaar, G. A.; Ballester, P.; de Mendoza, J. *New J. Chem.* **2009**, *33*, 777.

32. Shetti, V. S.; Ravikanth, M. *Inorg. Chem.* 2011, *50,* 1713.

33. Pareek, Y.; Ravikanth, M. *J. Organomett. Chem.* **2013**, *724*, 67-74.

34. Wan, C. W.; Burghart, A.; Chen, J.; Bergström, F.; Johansson, L. B. Å.; Wolford, M. F.; Kim, T. G.; Topp, M. R.; Hochstrasser, R. M.; Burgess, K. *Chem. Eur. J.* **2003**, *9*, 4430-

4441.

35. Pareek, Y.; Ravikanth, M. *Eur. J. Org. Chem.* **2011**, *27*, 5390-5399.

36. Shetti, V. S.; Ravikanth, M. *J. Porphyrins Phthalocyanines* **2010**, *14*, 361.

37. Gupta, I.; Ravikanth, M. *Inorg. Chim. Acta* **2007**, *360*, 1731–1742.

## Legends

**Chart 1:** Molecular structures of pentads **1-3**.

**Scheme 1:** Synthesis of dyads **4-6**.

**Scheme 2:** Synthesis of pentads **1-3**.

**Figure 1:** Comparison of $^1$H NMR of (i) BODIPY-porphyrin dyad **5** with its corresponding monomers (ii) **9** and (iii) **7**.

**Figure 2:** Comparison of $^1$H NMR spectrum of (i) pentad **1** along with its constituted (ii) Sn(IV) porphyrin monomer **11** and (iii) dyad **4**. $^1$H-$^1$H COSY spectrum shows connectivity between 2,6 and 3,5 aryl protons.

**Figure 3:** Comparison of Q-band and Soret band (inset) absorption spectra of (a) pentad **1**, (b) pentad **2**, and (c) pentad **3** (solid line), along with 1:1 mixture (dotted line) of their corresponding dyad and Sn(IV) porphyrin monomer.

**Figure 4:** Reduction waves of cyclic voltammograme (solid line) and diferential pulse voltammograme (dotted line) of (i) pentad **2** (a), SnTTP **11** (b) and dyad **5** (c) and (ii) pentad **3** (a), SnTTP **11** (b) and dyad **6** (c) recorded in dichloromethane containing 0.1 M TBAP as supporting electrolyte (scan rate 50 mV/sec).

**Figure 5:** Emission spectrum of (a) pentad **1**, (b) pentad **2** and (c) pentad **3** (solid line) along with 1:1 mixture (dotted line) of their corresponding dyad and Sn(IV) porphyrin monomer recorded at excitation wavelength of 560 nm.

**Table 1.** Absorption data for the pentads **1, 2** and **3** along with their corresponding dyads **4-6** and other monomeric unit.

**Table 2.** Redox data for pentads **1-3** and their constituted dyads **4-6** with their corresponding monomeric units.

**Table 3:** Photophysical data for pentads **1-3** and their constituted dyads **4-6**.

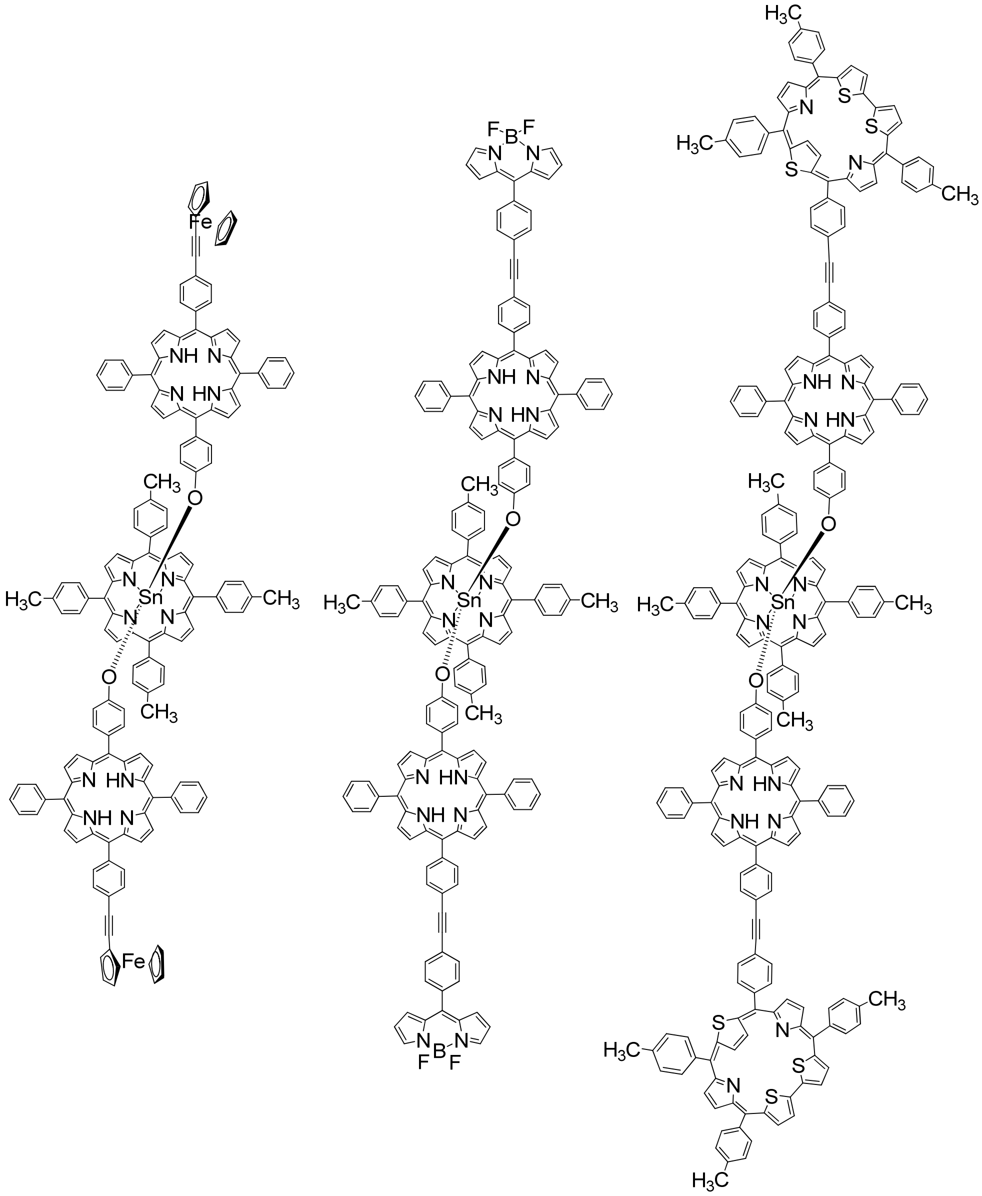

Chart 1

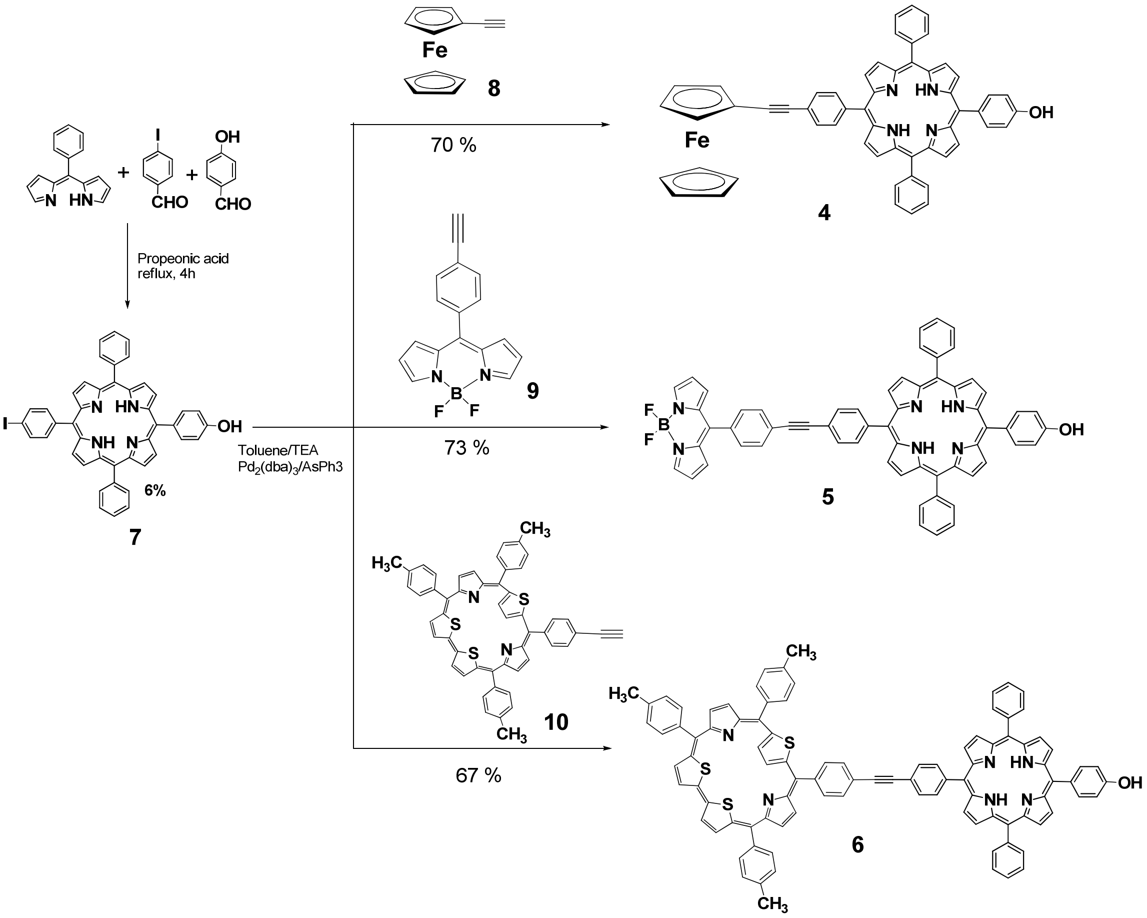
Fe
8
70 %
Fe
OH
4
Propeonic acid
reflux, 4h
OH
I
+
+
CHO
CHO
N
HN
9
N
B
N
F
F
I
OH
6%
7
Toluene/TEA
$Pd_2(dba)_3$/AsPh3
73 %
F
B
F
N
N
OH
5
$CH_3$
$H_3C$
S
S
N
N
S
10
$CH_3$
67 %
$CH_3$
$H_3C$
OH
6
$CH_3$
NH
HN

Scheme 1

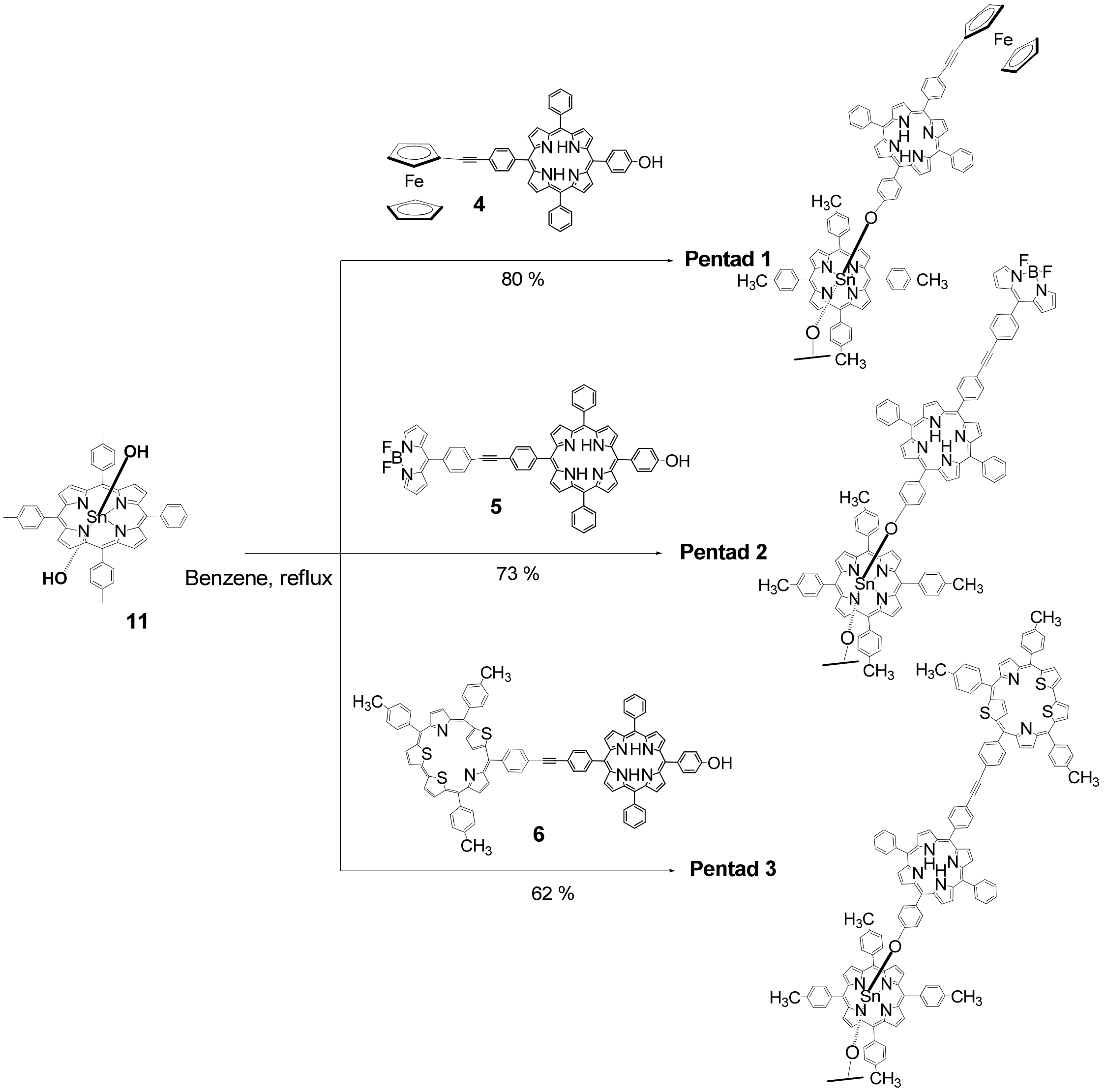

Scheme 2

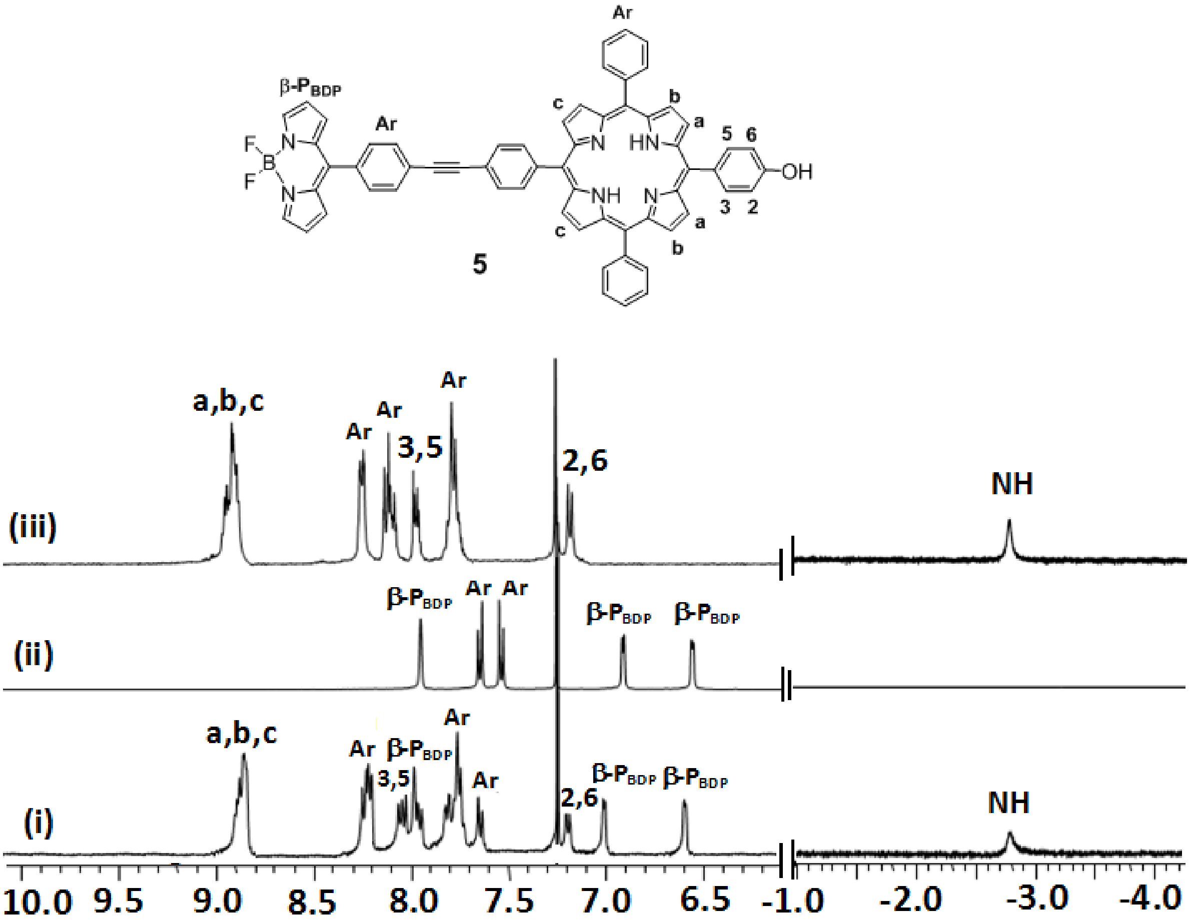
Ar
β-P$_{BDP}$
Ar
c
b
a
5 6
OH
3 2
N
HN
NH
N
F
B
F
N
N
a
b
c
5
a,b,c
Ar
Ar
Ar
3,5
2,6
NH
(iii)
β-P$_{BDP}$
Ar Ar
β-P$_{BDP}$ β-P$_{BDP}$
(ii)
a,b,c
Ar β-P$_{BDP}$
3,5
Ar
Ar
β-P$_{BDP}$ β-P$_{BDP}$
2,6
NH
(i)
10.0 9.5 9.0 8.5 8.0 7.5 7.0 6.5 -1.0 -2.0 -3.0 -4.0

Figure 1

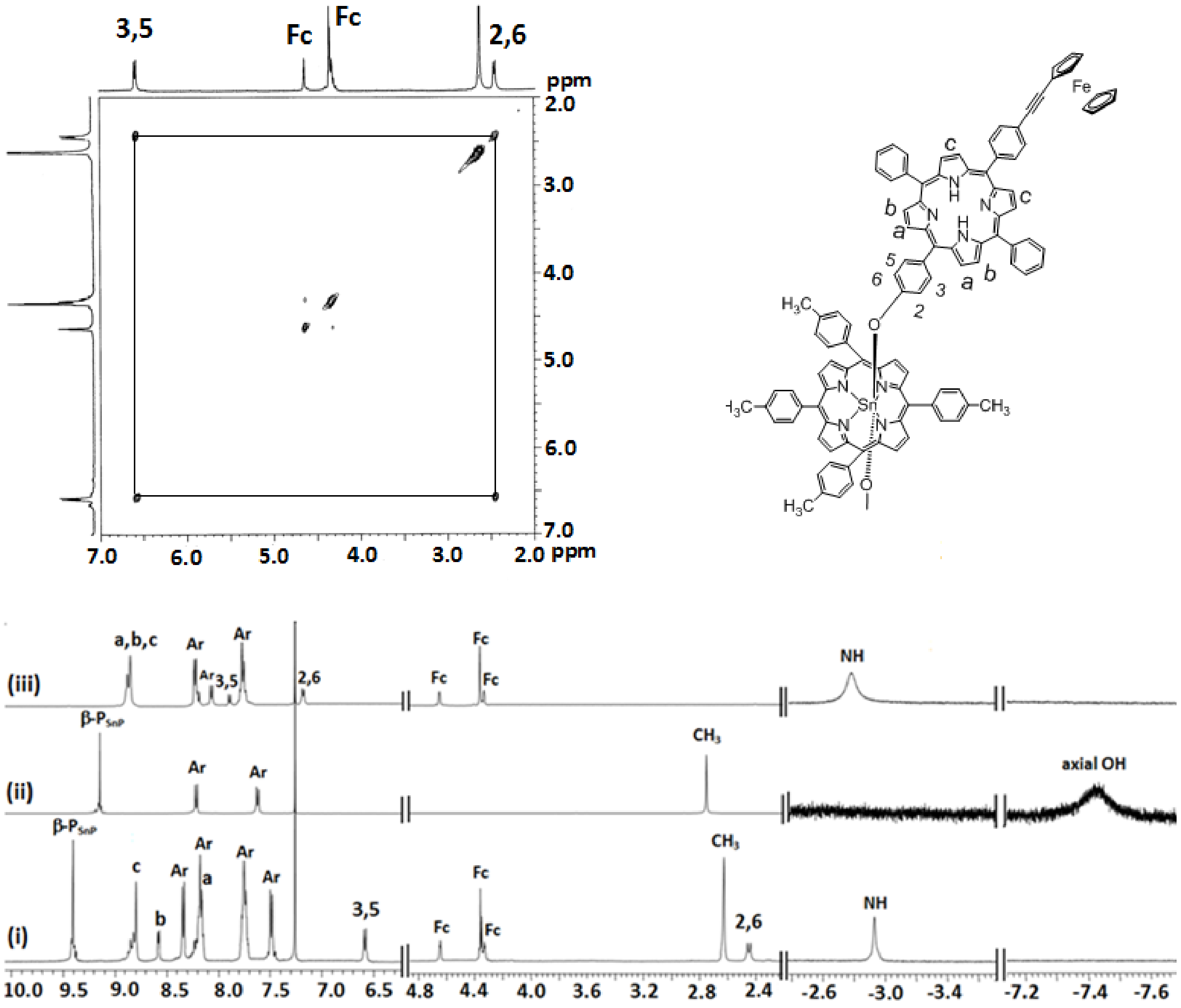
3,5
Fc
Fc
2,6
ppm
2.0
3.0
4.0
5.0
6.0
7.0
7.0
6.0
5.0
4.0
3.0
2.0 ppm
Fe
c
c
b
a
b
a
5
6
3
2
H
N
N
H
N
N
O
Sn
N
N
N
N
O
$H_3C$
$H_3C$
$CH_3$
$H_3C$
(iii)
a,b,c
Ar
Ar
Ar
3,5
2,6
Fc
Fc
Fc
NH
(ii)
β-P<sub>SnP</sub>
Ar
Ar
$CH_3$
axial OH
(i)
β-P<sub>SnP</sub>
c
b
Ar
Ar
a
Ar
Ar
3,5
Fc
Fc
Fc
$CH_3$
2,6
NH
10.0
9.5
9.0
8.5
8.0
7.5
7.0
6.5
4.8
4.4
4.0
3.6
3.2
2.8
2.4
-2.6
-3.0
-3.4
-7.2
-7.4
-7.6

Figure 2

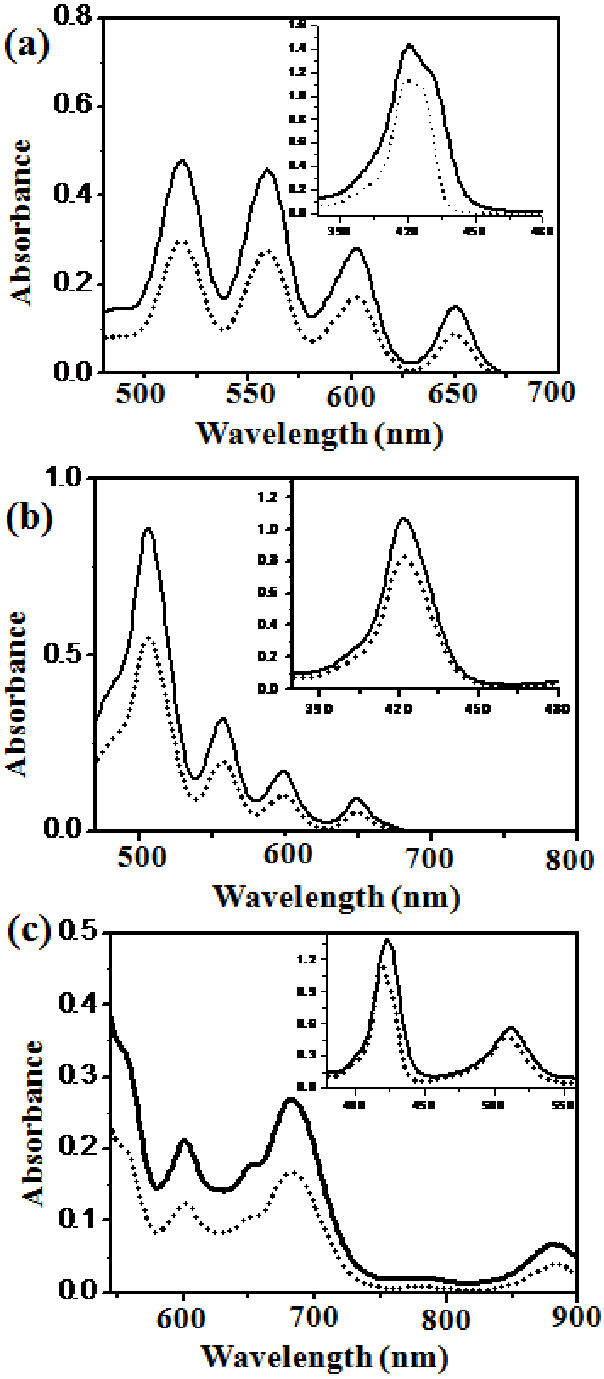
(a)
Absorbance
0.0
0.2
0.4
0.6
0.8
500
550
600
650
700
Wavelength (nm)
(b)
Absorbance
0.0
0.5
1.0
500
600
700
800
Wavelength (nm)
(c)
Absorbance
0.0
0.1
0.2
0.3
0.4
0.5
600
700
800
900
Wavelength (nm)

Figure 3

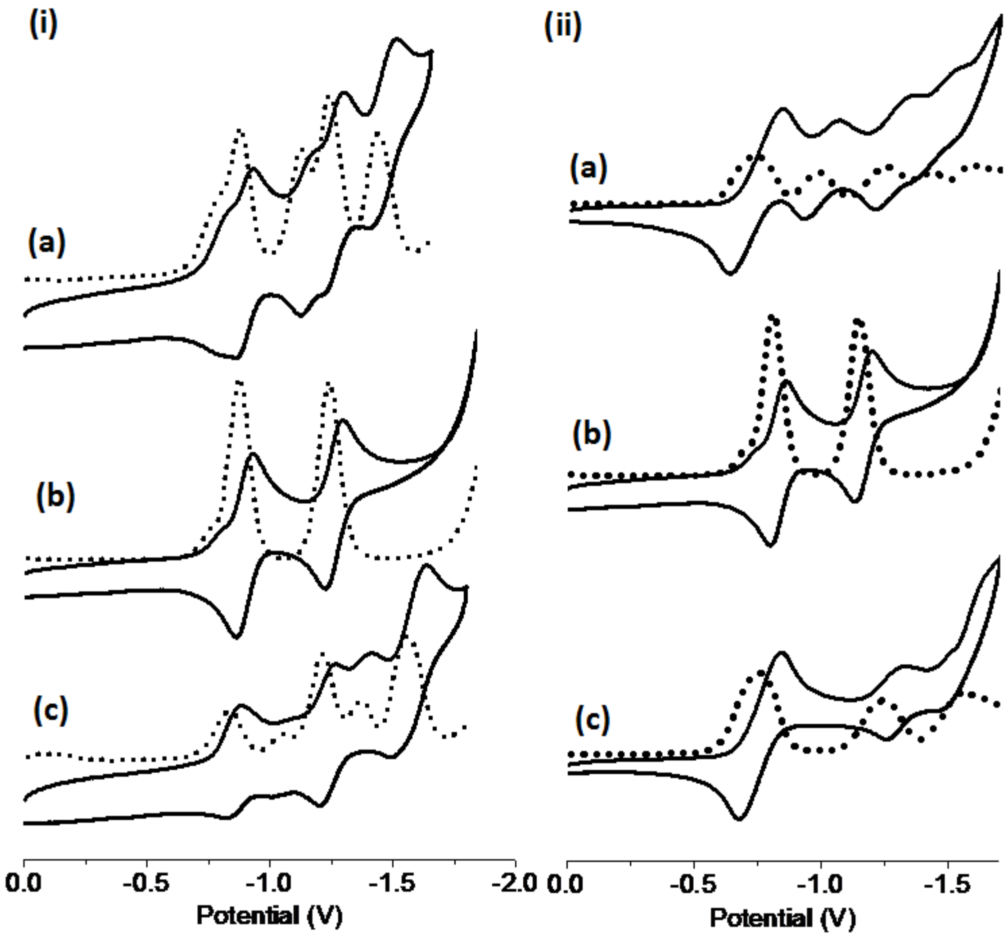

Figure 4

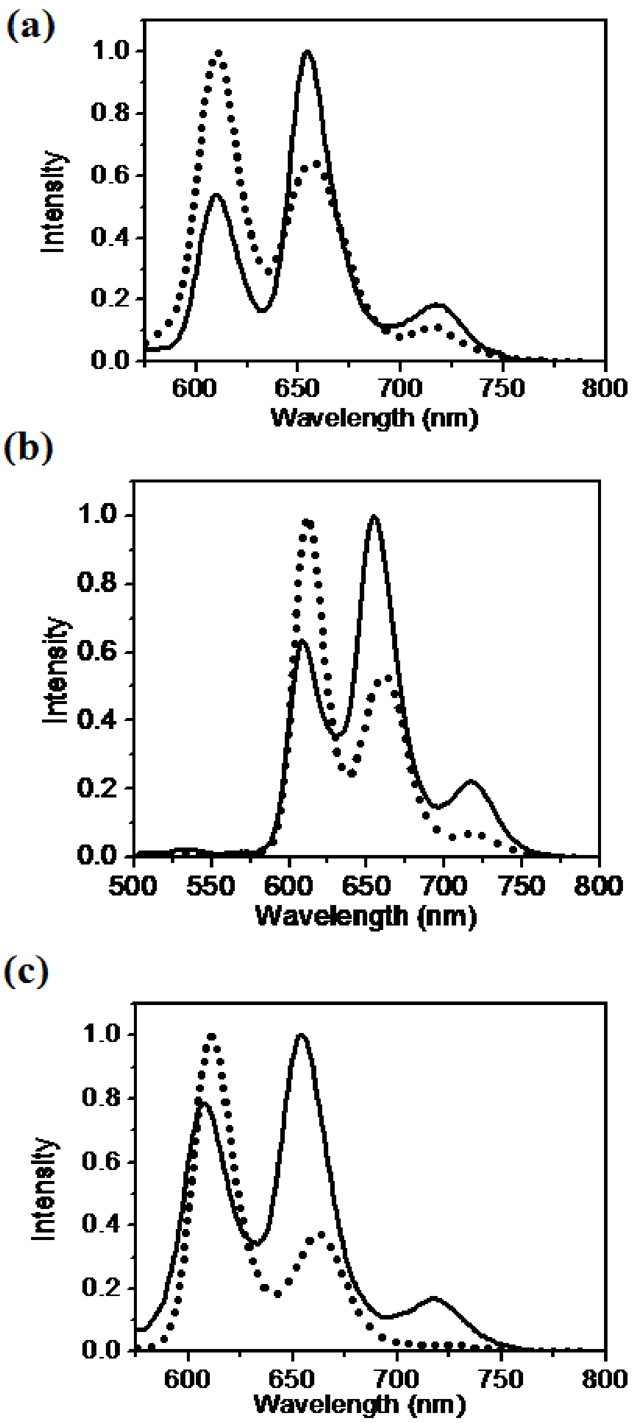
(a)
Intensity
1.0
0.8
0.6
0.4
0.2
0.0
600
650
700
750
800
Wavelength (nm)
(b)
Intensity
1.0
0.8
0.6
0.4
0.2
0.0
500
550
600
650
700
750
800
Wavelength (nm)
(c)
Intensity
1.0
0.8
0.6
0.4
0.2
0.0
600
650
700
750
800
Wavelength (nm)

Figure 5

## Table 1

| Compd. No. | Soret band λ [nm] (log ε) | Q bands λ [nm] (log ε) | | | | | |
|---|---|---|---|---|---|---|---|
| **11** | 427 (5.91) | - | 562 (4.51) | 603 (4.46) | - | - | - |
| **7** | 419 (6.18) | 516 (4.50) | 552 (4.26) | 592 (3.99) | 648 (4.05) | - | - |
| **9** | - | 503 (5.92) | - | - | - | - | - |
| **10** | 510 (5.74) | - | - | - | 627 (4.35) | 682 (4.70) | 880 (4.05) |
| **4** | 418 (6.24) | 516 (4.33) | 552 (4.06) | 592 (3.79) | 648 (3.86) | - | - |
| **5** | 420 (6.36) | 506 (4.71) | 552 (4.01) | 593 (3.70) | 649 (3.65) | - | - |
| **6** | 418 (5.31)<br>513 (4.33) | - | 550 (3.95) | 591 (3.73) | 647 (3.65) | 678 (3.56) | 882 (3.45) |
| **1** | 420 (6.15)<br>430 (6.08) | 517 (4.67) | 560 (4.65) | 602 (4.44) | 650 (4.17) | - | - |
| 2:1 mix. of **4** and **11** | 420 (6.05)<br>427 (6.02) | 516 (4.47) | 559 (4.44) | 602 (4.23) | 651 (3.93) | - | - |
| **2** | 421 (6.02)<br>431 (5.82) | 506 (4.93) | 557 (4.50) | 599 (4.22) | 649 (3.96) | - | - |
| 2:1 mix. of **5** and **11** | 419 (5.91)<br>430 (5.73) | 504 (4.74) | 556 (4.29) | 598 (4.01) | 650 (3.73) | - | - |
| **3** | 423 (6.13)<br>429 (6.06)<br>513 (5.74) | - | 555 (sh) | 601 (4.32) | 651 (4.24) | 682 (4.42) | 882 (3.83) |
| 2:1 mix. of **6** and **11** | 419 (6.06)<br>427 (5.92)<br>512 (5.68) | - | 556 (sh) | 601 (4.09) | 650 (4.02) | 683 (4.22) | 883 (3.60) |

## Table 2

| Compd. No. | Oxidation | | | | | | Reduction | | | | |
|---|---|---|---|---|---|---|---|---|---|---|---|
| | $E_{1/2}$/V vs. SCE | | | | | | $E_{1/2}$/V vs. SCE | | | | |
| $H_2TTP$ | - | 1.03 | | 1.30 | - | - | - | - | -1.23 | | -1.55 |
| $SnTTP(OH)_2$ | - | - | | - | 1.42 | - | - | -0.97 | - | -1.36 | - |
| **8** | 0.62 | - | | - | - | - | - | - | - | | |
| **4** | 0.62 | 1.03 | | 1.30 | - | | | | -1.23 | | -1.55 |
| **1** | 0.59 | 1.00 | | - | 1.41 | - | | -0.90 | -1.26 | -1.39 | -1.58 |
| **9** | - | - | | - | - | - | -0.74 | - | - | - | -1.58 |
| **5** | - | 0.99 | | 1.32 | - | - | -0.78 | | -1.25 | - | -1.54 |
| **2** | - | 1.01 | | 1.27 | 1.42 | - | -0.73 | -0.99 | -1.25 | -1.40 | -1.58 |
| **10** | 0.74 | - | 1.17 | 1.39 | - | 1.60 | -0.87 | -1.09 | - | - | -1.55 |
| **6** | 0.71 | 0.94 | 1.10 | 1.26 | - | 1.60 | -0.85 | -1.05 | -1.29 | | -1.60 |
| **3** | 0.70 | 0.94 | 1.11 | 1.34 | 1.39 | 1.55 | -0.86 | -0.98 | -1.21 | -1.35 | -1.56 |

## Table 3

| Compound No. | $\lambda_{ex}$ (nm) | Sub-unit | $\Phi_M$ | $\Phi_{pentad}$ | % Quenching of chromophore |
|---|---|---|---|---|---|
| $SnTTP(OH)_2$ (**11**) | 560 | | 0.025 | - | - |
| $H_2TTP$ | 515 | | 0.11 | - | - |
| Rhodamine-6G | 488 | | 0.88 | - | - |
| **4** | 515 | $N_4$-Por. | - | 0.001 | 99 |
| **1** | 560 | Sn-Por. | - | 0.00079 | 97 |
| | | $N_4$-Por. | - | 0.0033 | 87 |
| | 515 | $N_4$-Por. | - | 0.026 | 77 |
| **5** | 488 | BODIPY | - | 0.0011 | 99.9 |
| | | $N_4$-Por. | - | 0.093 | |
| **2** | 488 | BODIPY | - | 0.0005 | 99.9 |
| | | $N_4$-Por. | - | 0.0005 | 95 |
| | 560 | Sn-Por. | - | 0.002 | 92 |
| | | $N_4$-Por. | - | 0.0035 | 86 |
| | 515 | $N_4$-Por. | - | 0.008 | 93 |
| **6** | 515 | $N_4$-Por. | - | 0.012 | 89 |
| **3** | 560 | Sn-Por. | - | 0.0045 | 82 |
| | | $N_4$-Por. | - | 0.0039 | 84 |
| | 515 | $N_4$-Por. | - | 0.0062 | 94 |

## Graphical Abstract

# Axial Bonded Pentads Constructed on Sn(IV) Porphyrin Scaffold

**Yogita Pareek, Vellanki Lakshmi and Mangalampalli Ravikanth**[*]

Department of Chemistry, Indian Institute of Technology Bombay, Powai,

Mumbai 400 076, India. E-mail: ravikanth@chem.iitb.ac.in

Three pentads based on Sn(IV) porphyrin scaffold were synthesized using three covalently linked dyads such as porphyrin-ferrocene, porphyrin-BODIPY and porphyrin-sapphyrin as an axial unit. The spectral, electrochemical and photophysical properties were studied for these dyads and pentads.